

Safety Embedded Stochastic Optimal Control of Networked Multi-Agent Systems via Barrier States

Lin Song¹, Pan Zhao¹, Neng Wan¹, and Naira Hovakimyan¹

Abstract—This paper presents a safe stochastic optimal control method for networked multi-agent systems (MASs) by using barrier states (BaSs) to embed the safety constraints into the system dynamics. The networked multi-agent system (MAS) is factorized into multiple subsystems, each of which is augmented with BaSs for the central agent. The optimal control law is obtained by solving the joint Hamilton-Jacobi-Bellman (HJB) equation on the augmented subsystem, which ensures safety via the boundedness of the BaSs. The BaS-based optimal control method generates safe control actions and also preserves optimality. The safe optimal control solution is ultimately approximated with path integrals. We validate the efficacy of the proposed approach in numerical simulations on a cooperative UAV team in two different scenarios.

I. INTRODUCTION

Optimal control has achieved great success in both theory and applications [1], [2]. Obtaining the optimal control is usually related to solving a nonlinear, second-order partial differential equation (PDE), called Hamilton-Jacobi-Bellman (HJB) equation. Stochastic optimal control (SOC) problems can be summarized as solving the control problem by minimizing an expected cost [3]. Under the exponential transformation of the value function [4], a linear-form HJB PDE is achieved, which facilitates related research including linearly-solvable optimal control (LSOC) [5] and path-integral control (PIC) [3], [6]. Benefits of LSOC problems include compositionality [7], [8] and path-integral representation of the optimal control solution. However, SOC solutions are challenging to compute in large-scale systems due to the curse of dimensionality [9]. To overcome the computational challenges, many approximation-based approaches including path-integral (PI) formulation [10], value function approximation [11], and policy approximation [12], have been established. In [13], a PI approach is applied to approximate the optimal control actions on multi-agent systems (MASs), and optimal path distribution is predicted via the graphical model inference approach. A distributed PIC algorithm is proposed in [14] such that a networked multi-agent system (MAS) is partitioned into multiple subsystems, from which local optimal control actions are determined with local observations. Nevertheless, the aforementioned approaches seldom consider safety in the problem formulation, which may limit their real-world applications.

Safety refers to ensuring that the system states stay within an appropriate region at all times for deterministic systems, or with a high probability for stochastic systems. Reachability analysis is a formal verification approach to prove safety and guarantee performance for dynamical systems [15], [16]. Hamilton-Jacobi (HJ) reachability analysis gives the initial states that the system needs to avoid to remain safe, as well as the associated optimal control [17]. However, the reachable set in reachability analysis is typically expensive to compute and thus prohibits their application to multi-agent and high-dimensional systems. To enable safe optimal control, safety metrics can also be incorporated into the optimal control framework, either as objectives or constraints. In [18], temporal logic specifications are used as constraints for safety enforcement in optimal control development. The control barrier function (CBF) also serves as a potent tool to enforce system safety by solving optimal control with constraints in a minimally invasive fashion [19]. CBF-based methods have also been extended to stochastic systems with high-probability guarantees [20]–[22]. A multi-agent CBF framework which generates collision-free controllers is discussed in [23], [24]. Furthermore, guaranteed safety-constraint satisfaction in the network system is achieved in [25] under a valid assume-guarantee contract and with CBFs implemented onto subsystems. However, the implementation of CBFs as safety filters into the control inputs generated by an optimal control law may ultimately hurdle the optimality and can be typically reactive to the given constraints. Furthermore, feasibility of the quadratic programming (QP) reduced by CBF-based methods is not always guaranteed until the very recent work in [26]. The barrier state (BaS) method is a novel methodology studied in [27], in which the stability analysis of BaS-augmented system encodes both stabilization and safety of the original system, and a potential conflict between control objectives and safety enforcement is avoided. In [28], discrete BaS (DBaS) is employed with differential dynamic programming (DDP) in trajectory optimization, and it has been shown that bounded DBaS implies the generation of safe trajectories. The DBaSs have also been integrated in importance sampling to improve sample efficiency in safety-constrained sampling-based control problems in [29].

Compared with CBF-based methods which solve constrained optimization to determine certified-safe control actions at each time step, BaS-based safe control formulates the problem without explicit constraints; the safety notion is embedded in the solution boundedness, and potential conflict between control performance and safety requirements is prevented. However, the methodology of addressing the

*This work is supported by Air Force Office of Scientific Research (AF-SOR) (award #FA9550-21-1-0411) and National Aeronautics and Space Administration (NASA) (awards #80NSSC22M0070 and #80NSSC17M0051).

¹Lin Song, Pan Zhao, Neng Wan, and Naira Hovakimyan are with the Department of Mechanical Science and Engineering, University of Illinois at Urbana-Champaign, Urbana, IL 61801 USA {linsong2, panzhao2, nengwan2, nhovakim}@illinois.edu

safety issues without sacrificing the optimality on networked MASs is still an open problem. In this paper, we propose a safety-embedded stochastic optimal control framework for networked MASs by using BaSs proposed in [27]. We follow the MAS framework considered in [30], [31], where each local agent computes the optimal control based on the local observations. However, [31] does not consider the safety problem, while [30] formulates the safety concern in the CBF framework and is potentially subject to the aforementioned issues. To tackle the safety-guarantee deficiency issue of optimal controls, we augment the dynamics of the central agent in each subsystem with BaSs that embed safety constraints, and then formulate the optimal control problem using the augmented dynamics. Bounded solutions to the revised optimal control problem automatically ensure safety by the characteristics of BaSs.

The rest of this paper is organized as follows: Section II introduces the preliminaries of formulating stochastic optimal control problems, and the construction of barrier states; Section III formulates the safety-embedded stochastic optimal control framework on MASs as well as the path integral formulation to approximate the solution; and Section IV provides numerical simulations in two scenarios to validate the efficacy of the proposed approach. Finally, section V concludes the paper and discusses the future research directions. Some notations used in this paper are defined as follows: We use $|\mathcal{S}|$ to denote the cardinality of a set \mathcal{S} , $\det(X)$ denotes the determinant of matrix X , $\text{tr}(X)$ denotes the trace of matrix X , $\nabla_x V$ and $\nabla_{xx}^2 V$ refer to the gradient and Hessian matrix of scalar-valued function V , and $\|v\|_M^2 := v^\top M v$ denotes the weighted square norm.

II. PRELIMINARIES AND PROBLEM FORMULATION

A. Stochastic optimal control problems

1) *MASs and factorial subsystems*: For a MAS with N homogeneous agents indexed by $\{1, 2, \dots, N\}$, we use a connected and undirected graph $\mathcal{G} = \{\mathcal{V}, \mathcal{E}\}$ to describe the networked MAS, where vertex $v_i \in \mathcal{V}$ denotes agent i , and undirected edge $(v_i, v_j) \in \mathcal{E}$ if agent i and j can communicate with each other. We denote the index set of all agents neighboring agent i as \mathcal{N}_i and then factorize one networked MAS into multiple subsystems $\bar{\mathcal{N}}_i = \mathcal{N}_i \cup \{i\}$, i.e., each of the factorial subsystems comprises a central agent and all its neighboring agents. Fig. 1 gives an illustrative example of the adopted factorization scheme. In Fig. 1, \bar{x}_i and \bar{u}_i denote the joint states and joint control actions of factorial subsystem $\bar{\mathcal{N}}_i$, respectively. The local control action

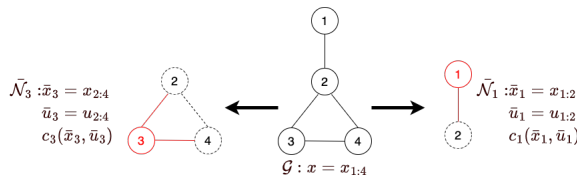


Fig. 1: MAS \mathcal{G} and factorial subsystems $\bar{\mathcal{N}}_1$ and $\bar{\mathcal{N}}_3$.

u_j depends on the local observation of agent j , i.e., \bar{x}_j ,

by minimizing a joint cost function of subsystem $\bar{\mathcal{N}}_j$. The complexities of computing local optimal control actions and sampling are then related to the size of each subsystem, instead of the entire network. More detailed discussions on the distributed control framework for LSOC problems on MASs can be found in [14].

2) *Stochastic optimal control of MASs*: For a networked MAS comprising N homogeneous agents, and governed by mutually independent passive dynamics, we use the following Itô diffusion process to describe the joint dynamics of subsystem $\bar{\mathcal{N}}_i$:

$$d\bar{x}_i = \bar{g}_i(\bar{x}_i, t)dt + \bar{B}_i(\bar{x}_i)[\bar{u}_i(\bar{x}_i, t)dt + \bar{\sigma}_i d\bar{\omega}_i], \quad (1)$$

where $\bar{x}_i = [x_i^\top, x_{j \in \mathcal{N}_i}^\top]^\top \in \mathbb{R}^{M \cdot |\bar{\mathcal{N}}_i|}$ is the joint state vector and M is the state dimension of each individual agent, $\bar{g}_i(\bar{x}_i, t) = [g_i(x_i, t)^\top, g_{j \in \mathcal{N}_i}(x_j, t)^\top]^\top \in \mathbb{R}^{M \cdot |\bar{\mathcal{N}}_i|}$ represents the joint passive dynamics, $\bar{B}_i(\bar{x}_i) = \text{diag}\{B_i(x_i), B_{j \in \mathcal{N}_i}(x_j)\} \in \mathbb{R}^{M \cdot |\bar{\mathcal{N}}_i| \times P \cdot |\bar{\mathcal{N}}_i|}$ is the joint control matrix, $\bar{u}_i(\bar{x}_i, t) = [u_i(\bar{x}_i, t)^\top, u_{j \in \mathcal{N}_i}(\bar{x}_i, t)^\top]^\top \in \mathbb{R}^{P \cdot |\bar{\mathcal{N}}_i|}$ is the joint control action vector, and $\bar{\omega}_i = [\omega_i^\top, \omega_{j \in \mathcal{N}_i}^\top]^\top \in \mathbb{R}^{P \cdot |\bar{\mathcal{N}}_i|}$ is the joint noise vector with the covariance matrix $\bar{\sigma}_i = \text{diag}\{\sigma_i, \sigma_{j \in \mathcal{N}_i}\} \in \mathbb{R}^{P \cdot |\bar{\mathcal{N}}_i| \times P \cdot |\bar{\mathcal{N}}_i|}$. We further assume that $\bar{g}_i, \bar{B}_i, \bar{\sigma}_i$ are locally Lipschitz continuous to guarantee the uniqueness of the solution.

We use $\bar{\mathcal{B}}_i$ to denote the set of joint terminal states, and $\bar{\mathcal{I}}_i$ denotes the set of joint non-terminal states, i.e., the entire allowable joint state space $\bar{\mathcal{S}}_i$ is partitioned into $\bar{\mathcal{I}}_i$ and $\bar{\mathcal{B}}_i$. We define the running cost function for $\bar{x}_i \in \bar{\mathcal{I}}_i$ as

$$c_i(\bar{x}_i, \bar{u}_i) = q_i(\bar{x}_i) + \frac{1}{2} \bar{u}_i(\bar{x}_i, t)^\top \bar{R}_i \bar{u}_i(\bar{x}_i, t),$$

where non-negative $q_i(\bar{x}_i) \in \mathbb{R}_{\geq 0}$ is a joint state cost, and $\bar{u}_i(\bar{x}_i, t)^\top \bar{R}_i \bar{u}_i(\bar{x}_i, t)$ is a control-quadratic cost with positive definite matrix $\bar{R}_i \in \mathbb{R}^{P \cdot |\bar{\mathcal{N}}_i| \times P \cdot |\bar{\mathcal{N}}_i|}$. When $\bar{x}_i^{t_f} \in \bar{\mathcal{B}}_i$, the terminal cost function is denoted by $\phi_i(\bar{x}_i^{t_f})$, and t_f is the final time. Particularly, we also have the terminal cost function $\phi_i(\bar{x}_i^{t_f})$ defined for $\bar{x}_i^{t_f} \in \mathcal{B}_i$. In the first exit formulation, t_f is determined online as the first time a joint state $\bar{x} \in \bar{\mathcal{B}}_i$ is reached. The cost-to-go function $J^{\bar{u}_i}(\bar{x}_i^t, t)$ under joint control action \bar{u}_i is defined as

$$J^{\bar{u}_i}(\bar{x}_i^t, t) = \mathbb{E}_{\bar{x}_i^t, t}^{\bar{u}_i} [\phi_i(\bar{x}_i^{t_f}) + \int_t^{t_f} c_i(\bar{x}_i(\tau), \bar{u}_i(\tau)) d\tau], \quad (2)$$

where the expectation is taken with respect to the probability measure under which \bar{x}_i satisfies (1) under given joint control action \bar{u}_i starting from the initial condition \bar{x}_i^t . The optimal cost-to-go function (or value function) is formulated as

$$V_i(\bar{x}_i^t, t) = \min_{\bar{u}_i} J^{\bar{u}_i}(\bar{x}_i^t, t),$$

and the value function is the minimum of expected cumulative running cost starting from joint state \bar{x}_i^t . In the following context, we suppress the state time-dependency in the notation, i.e., we denote $\bar{x}_i(t)$ or \bar{x}_i^t as \bar{x}_i for simplicity.

Facilitated by the exponential transformation of the value function, the optimal control action for stochastic system (1) is reduced to a linear form. The linear-form optimal control solution is introduced in [32] in the single-agent setting, and later discussed in the multi-agent scenario in [31]. We

briefly summarize the main results here. The desirability function over the joint state \bar{x}_i is defined as $Z(\bar{x}_i, t) = \exp[-V_i(\bar{x}_i, t)/\lambda_i]$, and the condition $\bar{\sigma}_i \bar{\sigma}_i^\top = \lambda_i \bar{R}_i^{-1}$ is satisfied to cancel the nonlinear terms. Then the linear-form joint optimal control action for the factorial subsystem $\bar{\mathcal{N}}_i$ in the networked MAS under aforementioned decentralization topology takes the form of

$$\bar{u}_i^*(\bar{x}_i, t) = \bar{\sigma}_i \bar{\sigma}_i^\top \bar{B}_i(\bar{x}_i)^\top \nabla_{\bar{x}_i} Z(\bar{x}_i, t) / Z(\bar{x}_i, t). \quad (3)$$

The nonlinearity cancellation condition essentially reflects the fact that control is expensive if one control channel has low noise variance, and thus large control effort is avoided.

Remark 1. In factorial subsystem $\bar{\mathcal{N}}_i$, we only obtain the local optimal control action $u_i^*(\bar{x}_i, t)$ for the central agent i , and local optimal control actions for the non-central agents $j(j \in \bar{\mathcal{N}}_i)$ in $\bar{\mathcal{N}}_i$ are computed from subsystem $\bar{\mathcal{N}}_j$.

B. Safety-embedded control via BaSs

The safety-embedded control methodology via BaSs is recently proposed in [27], [28], [33], which enforces the CBF constraints by constructing BaSs to augment the original system, and it has been shown that the boundedness of the BaSs implies the safety of the original system. We next briefly summarize the construction of BaS for nonlinear control-affine systems, which our proposed optimal control framework on the augmented MASs embedding safety builds upon. Consider nonlinear control-affine dynamical systems modeled as

$$\dot{x} = g(x) + b(x)u, \quad (4)$$

with $x \in \mathcal{D} \subset \mathbb{R}^M$, $u \in \mathbb{R}^P$, while $g : \mathbb{R}^M \rightarrow \mathbb{R}^M$, and $b : \mathbb{R}^M \rightarrow \mathbb{R}^{M \times P}$ are continuously differentiable functions. The set \mathcal{D} is domain of operation; we denote $h : \mathcal{D} \rightarrow \mathbb{R}$ as a continuously differentiable function representing the safe set, e.g., one safe operating region $\mathcal{C} := \{x \in \mathcal{D} | h(x) > 0\}$. One critical property of the scalar-valued barrier function (BF) $B(x)$ (e.g., inverse BF $B(x) = 1/h(x)$) is that its value remains bounded except when x approaches the boundaries of the safe operating region \mathcal{C} , i.e., as $h(x) \rightarrow 0$. Considering the composite barrier function (BF) in the form of $\beta(x) = B \circ h(x)$, where $h(x)$ defines a safe set, the dynamics of the BaS z are modeled as

$$\dot{z} = \phi_0(z + \beta_0)\dot{h}(x) - \gamma\phi_1(z + \beta_0, h(x)), \quad (5)$$

where $\beta_0 = \beta(0)$, $\dot{h}(x) = L_g h(x) + L_b h(x)u$, $\gamma \in \mathbb{R}_{>0}$, $\phi_0(\cdot), \phi_1(\cdot)$ are analytic functions formulated based on the choice of BF $B(\cdot)$, $h(x)$, and are also subject to certain conditions proposed in [27]. We next introduce a lemma from [27] which connects the boundedness of the BaSs with safety of the generated trajectories.

Lemma 1 ([27]). Suppose that $z(0) = \beta(x(0)) - \beta(0)$ and $\beta(x(0)) < \infty$, then the barrier state $z(t)$ generated from (5) with nonlinear dynamics (4) is bounded if and only if $\beta(x(t))$ is bounded $\forall t$.

Remark 2. From Lemma 1, we can observe that ensuring the boundedness of the BaS implies boundedness of $\beta(x(t))$, which further implies that $h(x(t)) > 0$ by properties of the

BF, and thus the system trajectories always remain in the safe operating region $\mathcal{C} = \{x \in \mathcal{D} | h(x) > 0\}$.

III. BARRIER STATE AUGMENTED STOCHASTIC OPTIMAL CONTROL OF MASS

A. Safe optimal control of MASs via BaSs

Based on the system factorization methodology introduced in Section II-A.1, we now formulate the safety-embedded optimal control on MASs using BaSs. As discussed in Remark 1 and the distributed control framework we build upon, since only agent i samples the local optimal control action from the computation results on subsystem $\bar{\mathcal{N}}_i$, we conjecture that it suffices to only append the BaSs corresponding to the central agent for each subsystem. One bounded solution to the optimal control problem on each subsystem certifies the safety of its included central agent, and taking certified-safe control actions for each agent from its corresponding subsystem (in which it acts as the central agent) collectively establishes safety of the entire network.

We first consider the local continuous-time dynamics of agent i within $\bar{\mathcal{N}}_i$ described by the following Itô process

$$dx_i = g_i(x_i, t)dt + B_i(x_i)[u_i(\bar{x}_i, t)dt + \sigma_i d\omega_i], \quad (6)$$

where $x_i \in \mathbb{R}^M$ denotes the state vector, $g_i(x_i, t) \in \mathbb{R}^M$ denotes the passive dynamics vector, $B_i(x_i) \in \mathbb{R}^{M \times P}$ denotes the control matrix, $u_i(\bar{x}_i, t) \in \mathbb{R}^P$ is the control action vector, and $\omega_i \in \mathbb{R}^P$ is the noise vector with covariance matrix $\sigma_i \in \mathbb{R}^{P \times P}$. The construction of the BaS introduced in Section II-B is based on general nonlinear control-affine dynamical systems. Here, we specifically consider the dynamics in form of (6) and construct the corresponding BaSs.

We use N_s independent BaSs to describe all the N_s interested safety constraints for each agent. For agent i , we denote the function modeling j -th constraint as $h_j(x_i)$, and denote the corresponding BaS associated with $h_j(x_i)$ as $z_{i(j)}$; suppose we use the inverse BF, i.e., $\beta(x_i) = 1/h(x_i)$, and we choose $\phi_0(\xi) = -\xi^2$, $\phi_1(\xi, \eta) = \eta\xi^2 - \xi$ as in [27]; then the dynamics for each single BaS are reduced to:

$$\begin{aligned} dz_{i(j)} = & [- (z_{i(j)} + \beta_{0(j)})^2 \left(\frac{\partial h_j}{\partial x_i} g_i(x_i, t) + \gamma h_j(x_i) \right) + \gamma (z_{i(j)} + \beta_{0(j)})] dt \\ & - (z_{i(j)} + \beta_{0(j)})^2 \frac{\partial h_j}{\partial x_i} B_i(x_i) [u_i(\bar{x}_i, t)dt + \sigma_i d\omega_i] \\ & := g_{bi(j)}(x_i, z_{i(j)}, t)dt + B_{bi(j)}(x_i, z_{i(j)})[u_i(\bar{x}_i, t)dt + \sigma_i d\omega_i], \end{aligned} \quad (7)$$

with $\beta_{0(j)} = 1/h_j(0)$, $z_{i(j)} \in \mathbb{R}$, $g_{bi(j)}(x_i, z_{i(j)}, t) \in \mathbb{R}$, $B_{bi(j)}(x_i, z_{i(j)}) \in \mathbb{R}^{1 \times P}$, and $u_i(\bar{x}_i, t) \in \mathbb{R}^P$. Since each agent is subject to N_s constraints, each of which is modeled by the BaS dynamics in (7), for agent i , the reorganized BaS dynamics for all the N_s constraints can be represented as

$$dz_i = g_{bi}(x_i, z_i, t)dt + B_{bi}(x_i, z_i)[u_i(\bar{x}_i, t)dt + \sigma_i d\omega_i], \quad (8)$$

with $z_i = [z_{i(1)}, \dots, z_{i(N_s)}]^\top \in \mathbb{R}^{N_s}$, $g_{bi}(x_i, z_i, t) = [g_{bi(1)}(x_i, z_i, t), \dots, g_{bi(N_s)}(x_i, z_i, t)]^\top \in \mathbb{R}^{N_s}$, $B_{bi}(x_i, z_i) = [B_{bi(1)}(x_i, z_i)^\top, \dots, B_{bi(N_s)}(x_i, z_i)^\top]^\top \in \mathbb{R}^{N_s \times P}$, and the individual elements $z_{i(j)}$, $g_{bi(j)}(x_i, z_i, t)$, and $B_{bi(j)}(x_i, z_i)$ are defined via (7). Considering the

joint continuous-time dynamics for factorial subsystem $\bar{\mathcal{N}}_i$ described by (1), we now integrate the BaS dynamics (8) corresponding to all the N_s constraints which the central agent i is subject to, and the augmented joint dynamics take the form of

$$d\bar{Y}_i = \bar{g}_i^\dagger(\bar{Y}_i, t)dt + \bar{B}_i^\dagger(\bar{Y}_i)[\bar{u}_i(\bar{Y}_i, t)dt + \bar{\sigma}_i d\bar{\omega}_i], \quad (9)$$

where the augmented joint state vector is $\bar{Y}_i = [x_i^\top, z_i^\top, x_{j \in \mathcal{N}_i}^\top]^\top := [Y_i^\top, x_{j \in \mathcal{N}_i}^\top]^\top \in \mathbb{R}^{M \cdot |\bar{\mathcal{N}}_i| + N_s}$, the augmented joint passive dynamics vector is $\bar{g}_i^\dagger(\bar{Y}_i, t) = [g_i(x_i, t)^\top, g_{bi}(x_i, z_i, t)^\top, g_{j \in \mathcal{N}_i}(x_j, t)^\top]^\top := [g_i^\dagger(Y_i, t)^\top, g_{j \in \mathcal{N}_i}(x_j, t)^\top]^\top \in \mathbb{R}^{M \cdot |\bar{\mathcal{N}}_i| + N_s}$, the augmented joint control matrix is $\bar{B}_i^\dagger(\bar{Y}_i) = \text{diag}\{B_i^\dagger(Y_i), B_{j \in \mathcal{N}_i}(x_j)\} \in \mathbb{R}^{(M \cdot |\bar{\mathcal{N}}_i| + N_s) \times (P \cdot |\bar{\mathcal{N}}_i|)}$ with $B_i^\dagger(Y_i) = [B_i(x_i)^\top, B_{bi}(x_i, z_i)^\top]^\top \in \mathbb{R}^{(M + N_s) \times P}$, $\bar{u}_i(\bar{Y}_i, t) = [u_i(\bar{x}_i, t)^\top, u_{j \in \mathcal{N}_i}(\bar{x}_i, t)^\top]^\top \in \mathbb{R}^{P \cdot |\bar{\mathcal{N}}_i|}$ is the joint control action for the augmented system, $\bar{\omega}_i = [\omega_i^\top, \omega_{j \in \mathcal{N}_i}^\top]^\top \in \mathbb{R}^{P \cdot |\bar{\mathcal{N}}_i|}$ is the joint noise vector, and $\bar{\sigma}_i = \text{diag}\{\sigma_i, \sigma_{j \in \mathcal{N}_i}\} \in \mathbb{R}^{(P \cdot |\bar{\mathcal{N}}_i|) \times (P \cdot |\bar{\mathcal{N}}_i|)}$ is the covariance matrix of noise vector $\bar{\omega}_i$. Particularly, $z_i = [z_i(1), z_i(2), \dots, z_i(N_s)]^\top \in \mathbb{R}^{N_s}$ is the BaS vector for agent i , and each of $z_i(j)$ is subject to (7). Since only some of the states are directly actuated, we can rearrange the states by partitioning the augmented joint state \bar{Y}_i into directly actuated states $\bar{Y}_{i(d)} \in \mathbb{R}^{D \cdot |\bar{\mathcal{N}}_i| + N_{SD}}$ and non-directly actuated states $\bar{Y}_{i(n)} \in \mathbb{R}^{U \cdot |\bar{\mathcal{N}}_i| + N_{SU}}$, and then $\bar{Y}_i = [\bar{Y}_{i(n)}^\top, \bar{Y}_{i(d)}^\top]^\top$, where U and D denote the dimension of the non-directly and directly actuated states for one agent, and N_{SU} , N_{SD} denote the dimension of non-directly and directly actuated BaSs for one agent. Then, the augmented joint dynamics in (9) can be rewritten in the following partitioned vector form

$$\begin{bmatrix} d\bar{Y}_{i(n)} \\ d\bar{Y}_{i(d)} \end{bmatrix} = \begin{bmatrix} \bar{g}_{i(n)}^\dagger(\bar{Y}_i, t) \\ \bar{g}_{i(d)}^\dagger(\bar{Y}_i, t) \end{bmatrix} dt + \begin{bmatrix} \mathbf{0} \\ \bar{B}_{i(d)}^\dagger(\bar{Y}_i) \end{bmatrix} [\bar{u}_i(\bar{Y}_i, t)dt + \bar{\sigma}_i d\bar{\omega}_i], \quad (10)$$

where $\mathbf{0}$ denotes a zero matrix with appropriate dimension. We define the joint running cost function of $\bar{\mathcal{N}}_i$ involving the augmented joint state \bar{Y}_i as

$$c_i(\bar{Y}_i, \bar{u}_i) = q_i(\bar{Y}_i) + \frac{1}{2} \bar{u}_i^\top(\bar{Y}_i, t) \bar{R}_i \bar{u}_i(\bar{Y}_i, t), \quad (11)$$

with $\bar{R}_i \in \mathbb{R}^{P \cdot \bar{\mathcal{N}}_i \times P \cdot \bar{\mathcal{N}}_i}$, which is positive definite. Here, we also assume that the control weights of each agent are decoupled, i.e., $\bar{R}_i = \text{diag}\{R_i, R_{j \in \mathcal{N}_i}\}$ and $\frac{1}{2} \bar{u}_i^\top \bar{R}_i \bar{u}_i = \sum_{j \in \mathcal{N}_i} \frac{1}{2} u_i R_i u_i$. Define the terminal cost function for the augmented joint state \bar{Y}_i as $\phi_i(\bar{Y}_i) = \sum_{j \in \mathcal{N}_i} \omega_j^i \phi_i(x_j) + \omega^i \phi_i(Y_i)$ with $\omega_j^i, \omega^i > 0$ denoting the weights reflecting the agent importance. The joint cost-to-go function subject to the control \bar{u}_i in the first-exit formulation for the augmented subsystem $\bar{\mathcal{N}}_i$ is defined as

$$J_i^{\bar{u}_i}(\bar{Y}_i^t, t) = \mathbb{E}_{\bar{Y}_i^t, t}^{\bar{u}_i} [\phi_i(\bar{Y}_i^{t_f}) + \int_t^{t_f} c_i(\bar{Y}_i(\tau), \bar{u}_i(\tau)) d\tau],$$

and the joint value function is defined as

$$V_i(\bar{Y}_i, t) = \min_{\bar{u}_i} \mathbb{E}_{\bar{Y}_i^t, t}^{\bar{u}_i} [\phi_i(\bar{Y}_i^{t_f}) + \int_t^{t_f} c_i(\bar{Y}_i(\tau), \bar{u}_i(\tau)) d\tau]. \quad (12)$$

We next introduce the optimal control that ensures safety can

be solved from a linear-form stochastic HJB equation, and summarize the result in the following theorem.

Theorem 1. Consider a MAS with N homogeneous agents with joint dynamics (1), the joint dynamics for subsystem $\bar{\mathcal{N}}_i$ that incorporate system safety by the central agent BaS augmentation are given by (9). Consider the augmented MAS, subject to joint immediate cost (11) and the joint value function (12), the joint optimal control action \bar{u}_{si}^* of subsystem $\bar{\mathcal{N}}_i$ ensuring safety is given by

$$\bar{u}_{si}^*(\bar{Y}_i, t) = -\bar{R}_i^{-1} \bar{B}_i^\dagger(\bar{Y}_i)^\top \nabla_{\bar{Y}_i} V_i(\bar{Y}_i, t). \quad (13)$$

Define the desirability function $Z_i(\bar{Y}_i, t) = \exp[-V_i(\bar{Y}_i, t)/\lambda_i]$, where $\lambda_i \in \mathbb{R}$, under the safe optimal control action (13) and nonlinearity cancellation condition $\bar{R}_i = (\bar{\sigma}_i \bar{\sigma}_i^\top / \lambda_i)^{-1}$, the joint stochastic HJB equation reduces to a linear form

$$\begin{aligned} \partial_t Z_i(\bar{Y}_i, t) &= [q_i(\bar{Y}_i) Z_i(\bar{Y}_i, t) / \lambda_i - \bar{g}_i^\dagger(\bar{Y}_i, t)^\top \nabla_{\bar{Y}_i} Z_i(\bar{Y}_i, t) \\ &\quad - \frac{1}{2} \text{tr}(\bar{B}_i^\dagger(\bar{Y}_i) \bar{\sigma}_i \bar{\sigma}_i^\top \bar{B}_i^\dagger(\bar{Y}_i)^\top \nabla_{\bar{Y}_i}^2 Z_i(\bar{Y}_i, t))], \end{aligned} \quad (14)$$

with boundary condition $\bar{Z}_i(\bar{Y}_i, t) = \exp[-\phi_i(\bar{Y}_i)/\lambda_i]$ and can be solved in a closed form as

$$Z_i(\bar{Y}_i, t) = \mathbb{E}_{\bar{Y}_i, t} [\exp(-\phi_i(\bar{p}_i^{t_f})/\lambda_i - \int_t^{t_f} q_i(\bar{p}_i)/\lambda_i d\tau)], \quad (15)$$

where the diffusion process $\bar{p}_i(t)$ is subject to the uncontrolled dynamics $d\bar{p}_i(\tau) = \bar{g}_i^\dagger(\bar{p}_i, \tau) d\tau + \bar{B}_i^\dagger(\bar{p}_i) \bar{\sigma}_i d\bar{\omega}_i$ with initial condition $\bar{p}_i(t) = \bar{Y}_i(t)$.

Remark 3. The proof of Theorem 1 is inspired by the proof of Theorem 2 in [14] with few modifications and observations.

i) Since the central agent states are now augmented with the BaSs while other agent states remain unchanged, we now need to differentiate the state-dependent terms in the value function between central and non-central agents for each subsystem; ii) Optimal control actions now take different forms for central and non-central agents, and the nonlinear term cancellation in the HJB equation needs to be considered separately with associated optimal control actions; iii) The safety property of the obtained optimal controls is established by the boundedness of the BaS, which is part of the augmented joint state. A feasible optimal control solution implies a bounded cost function, and thus bounded BaSs. For content completeness, we provide detailed derivation here.

Proof. We first substitute the immediate cost function (11) into (12), and denote s as a time step between t and t_f ; then

$$\begin{aligned} V_i(\bar{Y}_i, t) &= \min_{\bar{u}_i} \mathbb{E}_{\bar{Y}_i^t, t}^{\bar{u}_i} [V_i(\bar{Y}_i, s) + \int_t^s q_i(\bar{Y}_i) \\ &\quad + \frac{1}{2} \bar{u}_i^\top(\bar{Y}_i, \tau) \bar{R}_i \bar{u}_i(\bar{Y}_i, \tau) d\tau], \end{aligned}$$

which implies

$$\begin{aligned} 0 &= \min_{\bar{u}_i} \mathbb{E}_{\bar{Y}_i^t, t}^{\bar{u}_i} [(V_i(\bar{Y}_i, s) - V_i(\bar{Y}_i, t)) / (s - t) \\ &\quad + \frac{1}{s - t} \int_t^s q_i(\bar{Y}_i) + \frac{1}{2} \bar{u}_i^\top(\bar{Y}_i, \tau) \bar{R}_i \bar{u}_i(\bar{Y}_i, \tau) d\tau]. \end{aligned}$$

By letting $s \rightarrow t$, the optimality equation takes the form

$$0 = \min_{\bar{u}_i} \mathbb{E}_{\bar{Y}_i, t}^{\bar{u}_i} \left[\frac{dV_i(\bar{Y}_i, t)}{dt} + q_i(\bar{Y}_i) + \frac{1}{2} \bar{u}_i(\bar{Y}_i, t)^\top \bar{R}_i \bar{u}_i(\bar{Y}_i, t) \right]. \quad (16)$$

By expanding the $dV_i(\bar{Y}_i, t)/dt$ term using Itô's formula, and taking the expectation over all trajectories that initialized at (\bar{Y}_i^t, t) and subject to control \bar{u}_i , we have

$$\begin{aligned} \mathbb{E}_{\bar{Y}_i, t}^{\bar{u}_i} [dV_i(\bar{Y}_i, t)/dt] &= \partial V_i(\bar{Y}_i, t)/\partial t \\ &+ \sum_{j \in \mathcal{N}_i} [g_j(x_j, t) + B_j(x_j)u_j(\bar{Y}_i, t)]^\top \nabla_{x_j} V_i(\bar{Y}_i, t) \\ &+ [g_i^\dagger(Y_i, t) + B_i^\dagger(Y_i)u_i(\bar{Y}_i, t)]^\top \nabla_{Y_i} V_i(\bar{Y}_i, t) \\ &+ \frac{1}{2} \text{tr}(B_i^\dagger(Y_i)\sigma_i\sigma_i^\top B_i^\dagger(Y_i)^\top \nabla_{Y_i Y_i}^2 V_i(\bar{Y}_i, t)) \\ &+ \frac{1}{2} \sum_{j \in \mathcal{N}_i} \text{tr}(B_j(x_j)\sigma_j\sigma_j^\top B_j(x_j)^\top \nabla_{x_j x_j}^2 V_i(\bar{Y}_i, t)). \end{aligned} \quad (17)$$

Here, we use several identities: $\mathbb{E}_{\bar{Y}_i, t}^{\bar{u}_i} [dY_{i(m)}dx_{j(n)}] = (\sigma_i\sigma_i^\top)_{mm}\delta_{ij}\delta_{mn}dt$, $\mathbb{E}_{\bar{Y}_i, t}^{\bar{u}_i} [dY_{i(m)}dY_{i(n)}] = (\sigma_i\sigma_i^\top)_{mm}\delta_{mn}dt$, $\mathbb{E}_{\bar{Y}_i, t}^{\bar{u}_i} [dx_{j(m)}dx_{j(n)}] = (\sigma_j\sigma_j^\top)_{mm}\delta_{mn}dt$, where $(\cdot)_{mm}$ denotes the (m, m) entry of one matrix, and $\delta_{ij} = 1(0)$ if $i = j(i \neq j)$. Since $j \in \mathcal{N}_i$ and $j \neq i$, we have $\mathbb{E}_{\bar{Y}_i, t}^{\bar{u}_i} [dY_{i(m)}dx_{j(n)}] = 0$. Substituting (17) into (16) with above identities, the joint stochastic HJB equation for the augmented system is obtained as

$$\begin{aligned} -\partial_t V_i(\bar{Y}_i, t) &= \min_{\bar{u}_i} \mathbb{E}_{\bar{Y}_i, t}^{\bar{u}_i} [[g_i^\dagger(Y_i, t) + B_i^\dagger(Y_i)u_i(\bar{Y}_i, t)]^\top \nabla_{Y_i} V_i(\bar{Y}_i, t) \\ &+ \sum_{j \in \mathcal{N}_i} [g_j(x_j, t) + B_j(x_j)u_j(\bar{Y}_i, t)]^\top \nabla_{x_j} V_i(\bar{Y}_i, t) \\ &+ q_i(\bar{Y}_i) + \frac{1}{2} \bar{u}_i(\bar{Y}_i, t)^\top \bar{R}_i \bar{u}_i(\bar{Y}_i, t) \\ &+ \frac{1}{2} \text{tr}(B_i^\dagger(Y_i)\sigma_i\sigma_i^\top B_i^\dagger(Y_i)^\top \nabla_{Y_i Y_i}^2 V_i(\bar{Y}_i, t)) \\ &+ \frac{1}{2} \sum_{j \in \mathcal{N}_i} \text{tr}(B_j(x_j)\sigma_j\sigma_j^\top B_j(x_j)^\top \nabla_{x_j x_j}^2 V_i(\bar{Y}_i, t))], \end{aligned} \quad (18)$$

where the boundary condition is given by $V_i(\bar{Y}_i, t_f) = \phi_i(\bar{Y}_i)$. Since the RHS of (18) is quadratic in control, the safe optimal control action can be obtained by setting the derivatives of the operand with respect to $u_j(\bar{Y}_i, t)$ and $u_i(\bar{Y}_i, t)$ equal to zero, respectively, and we have

$$\begin{aligned} u_{\text{si}}^*(\bar{Y}_i, t) &= -R_i^{-1} B_i^\dagger(Y_i)^\top \nabla_{Y_i} V_i(\bar{Y}_i, t), \\ u_{\text{sj}}^*(\bar{Y}_i, t) &= -R_j^{-1} B_j(x_j)^\top \nabla_{x_j} V_i(\bar{Y}_i, t). \end{aligned} \quad (19)$$

With the exponential transformation of value function $Z_i(\bar{Y}_i, t) = \exp[-V_i(\bar{Y}_i, t)/\lambda_i]$, we can represent the terms involving $V_i(\bar{Y}_i, t)$ in (18) and (19) with respect to $Z_i(\bar{Y}_i, t)$. For each non-central agent $j \in \mathcal{N}_i$, by adopting the optimal control action u_{sj}^* , and according to the property of trace operator, we can simplify the terms in (18) as follows:

$$\begin{aligned} [B_j(x_j)u_j(\bar{Y}_i, t)]^\top \nabla_{x_j} V_i(\bar{Y}_i, t) &+ \frac{1}{2} u_j(\bar{Y}_i, t)^\top R_j u_j(\bar{Y}_i, t) \\ &= -\frac{\lambda_i^2}{2} \frac{\nabla_{x_j} Z_i(\bar{Y}_i, t)^\top B_j(x_j) R_j^{-1} B_j(x_j)^\top \nabla_{x_j} Z_i(\bar{Y}_i, t)}{Z_i^2(\bar{Y}_i, t)}, \end{aligned} \quad (20)$$

$$\begin{aligned} \frac{1}{2} \text{tr}(B_j(x_j)\sigma_j\sigma_j^\top B_j(x_j)^\top \nabla_{x_j x_j}^2 V_i(\bar{Y}_i, t)) \\ = -\lambda_i \text{tr}(B_j(x_j)\sigma_j\sigma_j^\top B_j(x_j)^\top \nabla_{x_j x_j}^2 Z_i(\bar{Y}_i, t))/2Z_i(\bar{Y}_i, t) \end{aligned}$$

$$+ \frac{\lambda_i \text{tr}(\nabla_{x_j} Z_i(\bar{Y}_i, t)^\top B_j(x_j)\sigma_j\sigma_j^\top B_j(x_j)^\top \nabla_{x_j} Z_i(\bar{Y}_i, t))}{2Z_i^2(\bar{Y}_i, t)}. \quad (21)$$

The quadratic terms on the desirability gradients in (20) and (21) are cancelled by selecting $\sigma_j\sigma_j^\top = \lambda_i R_j^{-1}$. Similarly, the quadratic terms with respect to the desirability gradients involving central agent i in (18) are cancelled by selecting $\sigma_i\sigma_i^\top = \lambda_i R_i^{-1}$, i.e., the nonlinearity cancellation condition can be further rewritten as $\bar{\sigma}_i\bar{\sigma}_i^\top = \lambda_i \bar{R}_i^{-1}$, and the linear-form stochastic HJB equation is thus obtained

$$\begin{aligned} \partial_t Z_i(\bar{Y}_i, t) &= \left[\frac{q_i(\bar{Y}_i)Z_i(\bar{Y}_i, t)}{\lambda_i} - \bar{g}_i^\dagger(\bar{Y}_i, t)^\top \nabla_{\bar{Y}_i} Z_i(\bar{Y}_i, t) \right. \\ &\quad \left. - \frac{1}{2} \text{tr}(\bar{B}_i^\dagger(\bar{Y}_i)\bar{\sigma}_i\bar{\sigma}_i^\top \bar{B}_i^\dagger(\bar{Y}_i)^\top \nabla_{\bar{Y}_i \bar{Y}_i}^2 Z_i(\bar{Y}_i, t)) \right], \end{aligned} \quad (22)$$

where the boundary condition is given by $Z_i(\bar{Y}_i, t_f) = \exp[-\phi_i(\bar{Y}_i)/\lambda_i]$. By invoking the Feynman-Kac formula, a solution to (22) can be formulated as

$$Z_i(\bar{Y}_i, t) = \mathbb{E}_{\bar{Y}_i, t} [\exp(-\phi_i(\bar{p}_i^{t_f})/\lambda_i - \int_t^{t_f} q_i(\bar{p}_i)/\lambda_i d\tau)],$$

where diffusion process $\bar{p}(t)$ satisfies $d\bar{p}_i(t) = \bar{g}_i^\dagger(\bar{p}_i, \tau) d\tau + \bar{B}_i^\dagger(\bar{p}_i)\bar{\sigma}_i d\bar{\omega}_i$ with the initial condition $\bar{p}_i(t) = \bar{Y}_i(t)$. ■

B. Path integral approximation formulation

Though the closed-form solution of the optimal control action is obtained in Theorem 1 of Section III-A, the expectation term over all trajectories initiated at (\bar{Y}_i^t, t) in the solution of the desirability function (15) is typically intractable to compute. We formulate the optimal control solution of the augmented system in path integrals and next introduce a proposition revised from Proposition 3 in [14].

Proposition 1. *Based on the partition of augmented joint state \bar{Y}_i into directly actuated states and non-directly actuated states as introduced in (10), we can further partition the time interval $[t, t_f]$ into K equal-length ($\varepsilon = (t_f - t)/K$) intervals, i.e., $t = t_0 < t_1 < t_2 < \dots < t_K = t_f$, and use the trajectory variables $\bar{Y}_i^{(k)} = [\bar{Y}_{i(n)}^{(k)\top}, \bar{Y}_{i(d)}^{(k)\top}]^\top$ to denote the joint uncontrolled ($\bar{u}_i(\bar{Y}_i, t) = 0$) trajectories of the augmented system on time $[t_{k-1}, t_k]$ with initial condition $\bar{Y}_i(t) = \bar{Y}_i^{(0)}$. We use $\bar{l}_i = (\bar{Y}_i^{(1)}, \bar{Y}_i^{(2)}, \dots, \bar{Y}_i^{(K)})$ to denote the path variable, and the generalized path value is formulated as*

$$\begin{aligned} \tilde{S}_i^{\varepsilon, \lambda_i}(\bar{Y}_i^{(0)}, \bar{l}_i, t_0) &= \frac{\phi_i(\bar{Y}_i^{(k)})}{\lambda_i} + \frac{\varepsilon}{\lambda_i} \sum_{k=0}^{K-1} q_i(\bar{Y}_i^{(k)}) \\ &+ \frac{1}{2} \sum_{k=0}^{K-1} \log \det(H_i^{(k)}) + \frac{\varepsilon}{2\lambda_i} \sum_{k=0}^{K-1} \|\alpha_i^{(k)}\|_{(H_i^{(k)})^{-1}}^2, \end{aligned} \quad (23)$$

with $H_i^{(k)} = \bar{B}_{i(d)}^\dagger(\bar{Y}_i^{(k)})\bar{\sigma}_i\bar{\sigma}_i^\top \bar{B}_{i(d)}^\dagger(\bar{Y}_i^{(k)})^\top$ and $\alpha_i^{(k)} = (\bar{Y}_{i(d)}^{(k+1)} - \bar{Y}_{i(d)}^{(k)})/\varepsilon - \bar{g}_{i(d)}^\dagger(\bar{Y}_i^{(k)}, t_k)$. Then, the joint optimal control action ensuring safety in subsystem $\bar{\mathcal{N}}_i$ in (13) can be formulated as path integral

$$\begin{aligned} \bar{u}_{\text{si}}^*(\bar{Y}_i, t) &= \\ \lambda_i \bar{R}_i^{-1} \bar{B}_{i(d)}^\dagger(\bar{Y}_i)^\top \cdot \lim_{\varepsilon \downarrow 0} \int \tilde{p}_i^*(\bar{l}_i | \bar{Y}_i^{(0)}, t_0) \cdot \tilde{u}_i(\bar{Y}_i^{(0)}, \bar{l}_i, t_0) d\bar{l}_i, \end{aligned}$$

where

$$\tilde{p}_i^*(\bar{l}_i|\bar{Y}_i^{(0)}, t_0) = \frac{\exp(-\tilde{S}_i^{\varepsilon, \lambda_i}(\bar{Y}_i^{(0)}, \bar{l}_i, t_0))}{\int \exp(-\tilde{S}_i^{\varepsilon, \lambda_i}(\bar{Y}_i^{(0)}, \bar{l}_i, t_0)) d\bar{l}_i}$$

is the optimal path distribution and

$$\begin{aligned} \tilde{u}_i(\bar{Y}_i^{(0)}, \bar{l}_i, t_0) = & -\frac{\varepsilon}{\lambda_i} \nabla_{\bar{Y}_i^{(0)}} q_i(\bar{Y}_i^{(0)}) \\ & + (H_i^{(0)})^{-1} ((\bar{Y}_i^{(1)} - \bar{Y}_i^{(0)})/\varepsilon - \bar{g}_{i(d)}^\dagger(\bar{Y}_i^{(0)}, t_0)) \end{aligned}$$

is the initial control variable.

Remark 4. Once feasible solutions to the cost-minimization problem (i.e., (12)) for the BaS-augmented subsystems are determined, which is expressed in a closed form in Theorem 1 and approximated in Proposition 1, the cost function must be bounded. Since the BaSs are also part of the cost function, the resulting BaSs are bounded. (Rigorously, the BaS boundedness is established in a mean-square sense, and the achieved safety is also in a mean-square sense). According to Lemma 1 and Remark 2, the achieved optimal control action to the augmented subsystem ensures safety of the central agent within the original subsystem. Taking safe optimal control actions for agent i from individual subsystem \mathcal{N}_i then collectively ensures safety of the entire network.

IV. SIMULATION RESULTS

In this section, we perform numerical simulations on cooperative MASs (a cooperative UAV team) in environments with both simple obstacles and more-challenging obstacles, with the goal of reaching targets, avoiding obstacles, and cooperating with other agents. Each UAV is subject to the continuous-time dynamics as follows:

$$\begin{pmatrix} dx_i \\ dy_i \\ dv_i \\ d\varphi_i \end{pmatrix} = \begin{pmatrix} v_i \cos \varphi_i \\ v_i \sin \varphi_i \\ 0 \\ 0 \end{pmatrix} dt + \begin{pmatrix} 0 & 0 \\ 0 & 0 \\ 1 & 0 \\ 0 & 1 \end{pmatrix} \left[\begin{pmatrix} u_i \\ w_i \end{pmatrix} dt + \begin{pmatrix} \sigma_i & 0 \\ 0 & \nu_i \end{pmatrix} d\omega_i \right], \quad (24)$$

where (x_i, y_i) , v_i , φ_i represent the position coordinate, forward velocity, and heading angle of UAV i . We use $\mathbf{x}_i := (x_i, y_i, v_i, \varphi_i)^\top$ to denote the state vector; the forward acceleration u_i and angular velocity w_i are the control inputs, and ω_i is the standard Brownian motion disturbance. We implement the simulations with the noise level of $\sigma_i = 0.1$ and $\nu_i = 0.05$; we also specify the exit time $t_f = 20$ seconds.

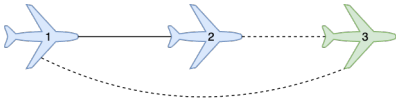


Fig. 2: A networked UAV team with UAVs 1 and 2 flying cooperatively and UAV 3 flying independently.

In all the following simulation examples, we adopt the safe optimal control action (13) introduced in Theorem 1 and approximate it using the path-integral formulation discussed in Proposition 1. We only sample local safe optimal control action for each central agent from the computed joint control actions in each subsystem. In the obstacle-avoidance tasks, we first model all the safety constraints with independent BaSs and then augment the joint dynamics for subsystems with the central agent BaSs' dynamics.

A. Passing through simple obstacles

In this example, we consider a cooperative UAV team as illustrated in Fig. 2, where UAVs 1 and 2 fly together with distance-minimized and UAV 3 flies independently. Initial position coordinates for UAVs 1, 2, and 3 are selected as $(5, 5)$, $(5, 45)$, and $(5, 25)$, respectively. The dotted lines in Fig. 2 represent the coordination between UAVs is not considered in designing the running cost function, and the UAVs are loosely-coupled; while the UAVs connected by a solid line can cooperate. The target position coordinates for the three UAVs are set identically as $(45, 25)$. Each UAV is governed by the continuous-time dynamics (24). We consider three circular obstacles in the environment modeled by $h_1(\mathbf{x}) = (x - 17)^2 + (y - 40)^2 - 8^2$, $h_2(\mathbf{x}) = (x - 22)^2 + (y - 16)^2 - 7^2$, $h_3(\mathbf{x}) = (x - 35)^2 + (y - 30)^2 - 5^2$, and the safe region is described by $\bar{\mathcal{C}} = \cap_{i=1}^3 \mathcal{C}_i$ with $\mathcal{C}_i := \{\mathbf{x} \in \mathbb{R}^2 : h_i(\mathbf{x}) > 0\}$. We use independent BaSs to represent the constraints for the central agent in each subsystem, and the BaS corresponding to constraint j for agent i is represented as z_{ij} and generated by (7). Particularly, as discussed in Lemma 1, we also set $z_{ij}(0) = \beta_j(\mathbf{x}_i(0)) - \beta_j(0)$, where $\beta_j(\cdot)$ is the inverse BF. We set the γ -parameter in (7) to be 0.5, which regulates how fast the BaS returns to $\beta(\mathbf{x}_i) - \beta_0$ as discussed in [27].

We assume that the communication network of the UAV team is fully-connected, i.e., all the UAVs can sense the states of other UAVs. Based on the factorization topology introduced in Section II-A.1, the joint states of the three factorial subsystems are: $\bar{\mathbf{x}}_1 = [\mathbf{x}_1, \mathbf{x}_2, \mathbf{x}_3]^\top$; $\bar{\mathbf{x}}_2 = [\mathbf{x}_1, \mathbf{x}_2, \mathbf{x}_3]^\top$; $\bar{\mathbf{x}}_3 = [\mathbf{x}_1, \mathbf{x}_2, \mathbf{x}_3]^\top$, where $\mathbf{x}_i = [x_i, y_i, v_i, \varphi_i]^\top$ is the state variable vector. The running cost functions for the three subsystems are designed as $q(\bar{\mathbf{x}}_1) = 3.5(\|(x_1, y_1) - (x_1^{t_f}, y_1^{t_f})\|_2 - d_{11}^{\max}) + 1.4(\|(x_1, y_1) - (x_2, y_2)\|_2 - d_{12}^{\max}) + 0.5\|(z_{11}, z_{12}, z_{13}) - (z_{11}^{t_f}, z_{12}^{t_f}, z_{13}^{t_f})\|_2^2 + 50 \prod_{j=1}^3 \mathbb{I}(z_{1j} > 0.01)$, $q(\bar{\mathbf{x}}_2) = 3.5(\|(x_2, y_2) - (x_2^{t_f}, y_2^{t_f})\|_2 - d_{22}^{\max}) + 1.4(\|(x_2, y_2) - (x_1, y_1)\|_2 - d_{21}^{\max}) + 1.5\|(z_{21}, z_{22}, z_{23}) - (z_{21}^{t_f}, z_{22}^{t_f}, z_{23}^{t_f})\|_2^2 + 50 \prod_{j=1}^3 \mathbb{I}(z_{2j} > 0.01)$, $q(\bar{\mathbf{x}}_3) = 6(\|(x_3, y_3) - (x_3^{t_f}, y_3^{t_f})\|_2 - d_{33}^{\max}) + 0.5\|(z_{31}, z_{32}, z_{33}) - (z_{31}^{t_f}, z_{32}^{t_f}, z_{33}^{t_f})\|_2^2 + 50 \prod_{j=1}^3 \mathbb{I}(z_{3j} > 0.01)$, where $\|(x_i, y_i) - (x_i^{t_f}, y_i^{t_f})\|$ computes the distance to the target for UAV i , $\|(x_i, y_i) - (x_j, y_j)\|$ computes the distance between UAV i and j , d_{ij}^{\max} denotes the difference between initial position of UAV i to the target, and d_{ij}^{\max} denotes the initial distance between UAV i and j . Besides the BaS dependency in running cost functions, large BaSs are also penalized when the indicator function $\mathbb{I}(\cdot)$ is activated. We use a step size of $\Delta t = 0.05s$ and an exit time $t_f = 20s$ in the simulation.

We compare the safe optimal control via the BaS augmentation method with the original optimal control method, which only includes constraint-violation penalty in the cost function. We run 8 simulations with each method under identical initial conditions on the UAV team, and the result is illustrated in Fig. 3. We denote the trajectories for UAVs 1, 2, and 3 with red, blue, and green lines, respectively. The starting points for all UAVs are denoted by small circles,

and the target is represented by a cross mark. Both methods successfully drive the UAV team to the target. However, most of the executed trajectories of the original optimal control still collide with the surrounding obstacles, and safety is not guaranteed, while the proposed method always ensures safety by avoiding all the obstacles. We design UAVs 1 and 2 to fly together as one of our control objectives. In Fig. 3, we observe UAVs 1 (red line) and 2 (blue line) make attempt to minimize the distance between them with the proposed method, which is not achieved with the original optimal control method. The better coordination performance can be explained as the obstacle-collision penalty (usually large for safety concerns) in the cost function of original optimal control entangles the agent coordination objective. However, with the BaS-augmented safe optimal control, which essentially encodes the safety constraints into BaSs without introducing explicit obstacle-collision penalty terms, other control objectives are not sacrificed.

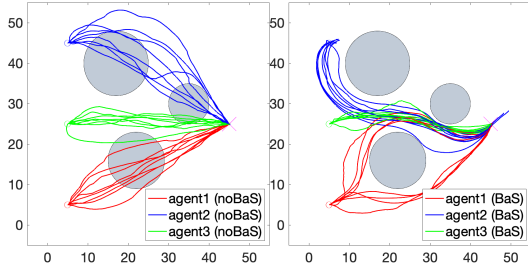


Fig. 3: Comparison between executed trajectories with original optimal control (left) and BaS-augmented safe optimal control (right) on a UAV team in environment with obstacles.

B. Passing through cluttered-obstacles

We further consider the same UAV team passing through a more obstacle-cluttered environment. The three UAVs are designed to fly from $(2.5, 2.5)$, $(2.5, 70)$, $(2.5, 40)$ to $(45, 45)$ while avoiding all the obstacles in the environment. We describe the five circular obstacles in the environment with following five functions: $h_1(\mathbf{x}) = (x - 15)^2 + (y - 3)^2 - 8^2$, $h_2(\mathbf{x}) = (x - 16)^2 + (y - 27)^2 - 8^2$, $h_3(\mathbf{x}) = (x - 27)^2 + (y - 15)^2 - 6^2$, $h_4(\mathbf{x}) = (x - 32.5)^2 + (y - 30.5)^2 - 12^2$, $h_5(\mathbf{x}) = (x - 20)^2 + (y - 60)^2 - 4^2$, and the safe region can be modeled as the intersection of the safe sets, i.e., $\bar{\mathcal{C}} = \cap_{i=1}^5 \mathcal{C}_i$ with $\mathcal{C}_i := \{\mathbf{x} \in \mathbb{R}^2 : h_i(\mathbf{x}) > 0\}$. We use the same γ and BaS-construction methodology as in the first experiment. The running cost functions for the three subsystems are now designed as $q(\bar{\mathbf{x}}_1) = 2(\|(x_1, y_1) - (x_1^{t_f}, y_1^{t_f})\|_2 - d_1^{\max}) + 0.5(\|(x_1, y_1) - (x_2, y_2)\|_2 - d_{12}^{\max}) + 0.8\|(z_{11}, z_{12}, z_{13}, z_{14}, z_{15}) - (z_{11}^{t_f}, z_{12}^{t_f}, z_{13}^{t_f}, z_{14}^{t_f}, z_{15}^{t_f})\|_2^2 + 24 \prod_{j=1}^5 \mathbb{I}(z_{1j} > 0.01)$, $q(\bar{\mathbf{x}}_2) = 2(\|(x_2, y_2) - (x_2^{t_f}, y_2^{t_f})\|_2 - d_2^{\max}) + 0.5(\|(x_2, y_2) - (x_1, y_1)\|_2 - d_{21}^{\max}) + 0.8\|(z_{21}, z_{22}, z_{23}, z_{24}, z_{25}) - (z_{21}^{t_f}, z_{22}^{t_f}, z_{23}^{t_f}, z_{24}^{t_f}, z_{25}^{t_f})\|_2^2 + 24 \prod_{j=1}^5 \mathbb{I}(z_{2j} > 0.01)$, $q(\bar{\mathbf{x}}_3) = 3(\|(x_3, y_3) - (x_3^{t_f}, y_3^{t_f})\|_2 - d_3^{\max}) + 0.8\|(z_{31}, z_{32}, z_{33}, z_{34}, z_{35}) - (z_{31}^{t_f}, z_{32}^{t_f}, z_{33}^{t_f}, z_{34}^{t_f}, z_{35}^{t_f})\|_2^2 + 48 \prod_{j=1}^5 \mathbb{I}(z_{3j} > 0.01)$. All the hyper-parameters (e.g., d_1^{\max}) follow the same definitions as in the first experiment.

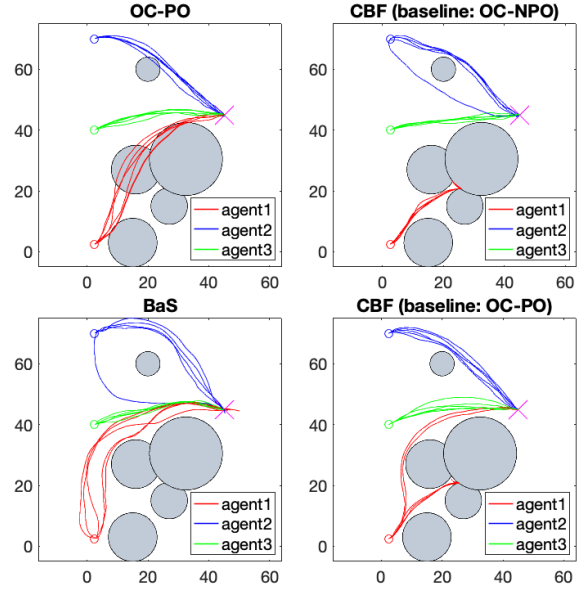


Fig. 4: Comparison of executed trajectories under optimal control penalizing obstacle-collision (top-left, abbreviation: ‘OC-PO’), CBF plus baseline optimal control without penalizing obstacle-collision (top-right, abbreviation: ‘CBF (baseline: OC-NPO)’), CBF plus baseline optimal control penalizing obstacle-collision (bottom-right, abbreviation: ‘CBF (baseline: OC-PO)’), and BaS-augmented optimal control (bottom-left) for a UAV team in an obstacle-cluttered environment.

We use a step size of $\Delta t = 0.2s$ and an exit time $t_f = 20s$ in the simulation.

We compute optimal control solutions for the goal-reaching, agent-coordinating, and obstacle-avoidance task using four different approaches. In the conventional optimal control framework, any violation of the safety constraints induces a penalty term in the cost function. The control barrier function (CBF)-based safe optimal controller, discussed in [22], [30], first solves a baseline optimal control, and then implements CBF as a safety filter to modify the baseline control input when necessary to ensure that the safety constraints are satisfied. Here, we further categorize the CBF-based safe optimal controller depending on whether the obstacle-collision penalty is considered in the baseline control cost function design. We compare these three methods with the BaS-based safe optimal control method proposed in this paper, which solves optimal control action on the joint dynamics with augmentation of the central agent BaSs. We run 5 simulations with each methods under identical initial conditions and the comparison results are shown in Fig. 4.

From Fig. 4, it is observed that the original optimal control obtained by simply penalizing constraint violation can still fail to avoid the obstacles in a cluttered environment. Furthermore, the CBF-based method that involves filtering the baseline optimal control by solving a quadratic programming (QP) problem at each time step, got trapped in the obstacles and failed to reach the target in some scenarios. The observed behavior is essentially due to the fact that CBF-based methods are reactive to the given safety constraints, and good tuning is necessary to ensure the feasibility and complete the

task. Finally, the proposed safe optimal control method using BaS augmentation ensures safety while successfully reaching the target and realizing desired coordination in all the trials.

V. CONCLUSION AND FUTURE WORK

In this paper, we propose a safety-embedded stochastic optimal control framework for networked MASs via barrier states (BaSs) augmentation. We first augment the joint dynamics of each factorial subsystem by introducing BaSs that embeds safety constraints for the central agent and then solve the optimal control action on the augmented subsystem. The proposed approach simultaneously ensures safety and other control objectives; where the former is guaranteed by the boundedness of BaSs and achieved by the feasible solutions to the reformulated optimal control problem. The safe optimal control law is obtained by solving a linear stochastic HJB equation, whose solution is ultimately approximated via the path-integral formulation. The proposed method is validated by numerical simulations on a networked UAV team. Future work includes representing the optimal control solution in policy improvement with path integrals (PI²) framework and other approximation formulations, e.g., Relative Entropy Policy Search (REPS). Additionally, the safety-embedded stochastic optimal control framework for MASs with incomplete state information is yet to be explored.

VI. ACKNOWLEDGMENT

The authors would like to appreciate the constructive discussions with Hassan Almubarak.

REFERENCES

- [1] D. Liberzon, *Calculus of Variations and Optimal Control Theory—A Concise Introduction*. NJ, USA: Princeton university press, 2011.
- [2] A. E. Bryson and Y.-C. Ho, *Applied Optimal Control: Optimization, Estimation, and Control*. Routledge, 2018.
- [3] H. J. Kappen, “Linear theory for control of nonlinear stochastic systems,” *Physical review letters*, vol. 95, no. 20, p. 200201, 2005.
- [4] E. Todorov, “Efficient computation of optimal actions,” *Proceedings of the national academy of sciences*, vol. 106, no. 28, pp. 11 478–11 483, 2009.
- [5] K. Dvijotham and E. Todorov, “Linearly solvable optimal control,” in *Reinforcement Learning and Approximate Dynamic Programming for Feedback Control*. Citeseer, 2012, vol. 17, pp. 119–141.
- [6] Y. Pan, E. Theodorou, and M. Kontitsis, “Sample efficient path integral control under uncertainty,” *Advances in Neural Information Processing Systems*, vol. 28, 2015.
- [7] E. Todorov, “Compositionality of optimal control laws,” *Advances in Neural Information Processing Systems*, vol. 22, 2009.
- [8] L. Song, N. Wan, A. Gahlawat, N. Hovakimyan, and E. A. Theodorou, “Compositionality of linearly solvable optimal control in networked multi-agent systems,” in *2021 American Control Conference (ACC)*. IEEE, 2021, pp. 1334–1339.
- [9] V. D. Blondel and J. N. Tsitsiklis, “A survey of computational complexity results in systems and control,” *Automatica*, vol. 36, no. 9, pp. 1249–1274, 2000.
- [10] E. Theodorou, J. Buchli, and S. Schaal, “A generalized path integral control approach to reinforcement learning,” *The Journal of Machine Learning Research*, vol. 11, pp. 3137–3181, 2010.
- [11] W. B. Powell and J. Ma, “A review of stochastic algorithms with continuous value function approximation and some new approximate policy iteration algorithms for multidimensional continuous applications,” *Journal of Control Theory and Applications*, vol. 9, no. 3, pp. 336–352, 2011.
- [12] R. S. Sutton, D. McAllester, S. Singh, and Y. Mansour, “Policy gradient methods for reinforcement learning with function approximation,” *Advances in Neural Information Processing Systems*, vol. 12, 1999.
- [13] B. Van Den Broek, W. Wiegierinck, and B. Kappen, “Graphical model inference in optimal control of stochastic multi-agent systems,” *Journal of Artificial Intelligence Research*, vol. 32, pp. 95–122, 2008.
- [14] N. Wan, A. Gahlawat, N. Hovakimyan, E. A. Theodorou, and P. G. Voulgaris, “Distributed algorithms for linearly-solvable optimal control in networked multi-agent systems,” *arXiv preprint arXiv:2102.09104*, 2021.
- [15] S. Summers and J. Lygeros, “Verification of discrete time stochastic hybrid systems: A stochastic reach-avoid decision problem,” *Automatica*, vol. 46, no. 12, pp. 1951–1961, 2010.
- [16] M. P. Chapman, J. Lacotte, A. Tamar, D. Lee, K. M. Smith, V. Cheng, J. F. Fisac, S. Jha, M. Pavone, and C. J. Tomlin, “A risk-sensitive finite-time reachability approach for safety of stochastic dynamic systems,” in *2019 American Control Conference (ACC)*. IEEE, 2019, pp. 2958–2963.
- [17] S. Bansal, M. Chen, S. Herbert, and C. J. Tomlin, “Hamilton-jacobi reachability: A brief overview and recent advances,” in *2017 IEEE 56th Annual Conference on Decision and Control (CDC)*. IEEE, 2017, pp. 2242–2253.
- [18] M. B. Horowitz, E. M. Wolff, and R. M. Murray, “A compositional approach to stochastic optimal control with co-safe temporal logic specifications,” in *2014 IEEE/RSJ International Conference on Intelligent Robots and Systems*. IEEE, 2014, pp. 1466–1473.
- [19] A. D. Ames, X. Xu, J. W. Grizzle, and P. Tabuada, “Control barrier function based quadratic programs for safety critical systems,” *IEEE Transactions on Automatic Control*, vol. 62, no. 8, pp. 3861–3876, 2016.
- [20] A. Clark, “Control barrier functions for stochastic systems,” *Automatica*, vol. 130, p. 109688, 2021.
- [21] M. Sarkar, D. Ghose, and E. A. Theodorou, “High-relative degree stochastic control lyapunov and barrier functions,” *arXiv preprint arXiv:2004.03856*, 2020.
- [22] A. Clark, “Control barrier functions for complete and incomplete information stochastic systems,” in *2019 American Control Conference (ACC)*. IEEE, 2019, pp. 2928–2935.
- [23] L. Wang, A. D. Ames, and M. Egerstedt, “Safety barrier certificates for collisions-free multirobot systems,” *IEEE Transactions on Robotics*, vol. 33, no. 3, pp. 661–674, 2017.
- [24] U. Borrmann, L. Wang, A. D. Ames, and M. Egerstedt, “Control barrier certificates for safe swarm behavior,” *IFAC-PapersOnLine*, vol. 48, no. 27, pp. 68–73, 2015.
- [25] Y. Chen, J. Anderson, K. Kalsi, A. D. Ames, and S. H. Low, “Safety-critical control synthesis for network systems with control barrier functions and assume-guarantee contracts,” *IEEE Transactions on Control of Network Systems*, vol. 8, no. 1, pp. 487–499, 2020.
- [26] W. Xiao, C. A. Belta, and C. G. Cassandras, “Sufficient conditions for feasibility of optimal control problems using control barrier functions,” *Automatica*, vol. 135, p. 109960, 2022.
- [27] H. Almubarak, N. Sadegh, and E. A. Theodorou, “Safety embedded control of nonlinear systems via barrier states,” *IEEE Control Systems Letters*, vol. 6, pp. 1328–1333, 2021.
- [28] H. Almubarak, K. Stachowicz, N. Sadegh, and E. A. Theodorou, “Safety embedded differential dynamic programming using discrete barrier states,” *IEEE Robotics and Automation Letters*, vol. 7, no. 2, pp. 2755–2762, 2022.
- [29] M. Gandhi, H. Almubarak, Y. Aoyama, and E. Theodorou, “Safety in augmented importance sampling: Performance bounds for robust mppi,” *arXiv preprint arXiv:2204.05963*, 2022.
- [30] L. Song, N. Wan, A. Gahlawat, C. Tao, N. Hovakimyan, and E. A. Theodorou, “Generalization of safe optimal control actions on networked multi-agent systems,” *IEEE Transactions on Control of Network Systems*, 2022.
- [31] N. Wan, A. Gahlawat, N. Hovakimyan, E. A. Theodorou, and P. G. Voulgaris, “Cooperative path integral control for stochastic multi-agent systems,” in *2021 American Control Conference (ACC)*. IEEE, 2021, pp. 1262–1267.
- [32] W. H. Fleming, “Exit probabilities and optimal stochastic control,” *Applied Mathematics and Optimization*, vol. 4, no. 1, pp. 329–346, 1977.
- [33] H. Almubarak, E. A. Theodorou, and N. Sadegh, “Barrier states embedded iterative dynamic game for robust and safe trajectory optimization,” in *2022 American Control Conference (ACC)*, 2022, pp. 5166–5172.